[논 문] 한국재료학회지
Korean Journal of Materials Research
Vol. 8, No. 12 (1998)

Fabrication of $YBa_2Cu_3O_{7-y}$-Ag Composite Superconductors by Pyrophoric Synthetic Method

Suk-Woo Yang, Chan-Joong Kim*, Gye-Won Hong* and Hyung-Shik Shin

Department of Chemical Engineering, Chonbuk National University, Chonju, Chonbuk, 560-756
**Superconductivity Research Laboratory, Korea Atomic Energy Research Institute, P.O. Box 105, Yusung, Taejon, 305-600*

발화합성법에 의한 $YBa_2Cu_3O_{7-y}$-Ag 복합 초전도체 제조

양석우 · 김찬중* · 홍계원* · 신형식
*한국원자력연구소 기능성재료연구팀
전북대학교 화학공학과

(1998년 3월 6일 받음, 1998년 10월 10일 최종수정본 받음)

초 록 $YBa_2Cu_3O_{7-y}$(123) 초전도체에서 은 입자의 미세분산을 얻고자 말릭산을 사용한 발화합성과 고상반응법으로 123와 123-Ag 복합 초전도분말을 제조하였다. 발화합성분말을 원료로 사용할 시 마이크론 미만의 미세한 123 분말과 은 분말의 복합체를 얻을 수 있었다. 원료로 사용된 산화은(Ag_2O) 분말은 발화합성과정 중 금속 은으로 환원되었다. 원료분말에 첨가된 금속 은에 의한 반응 물질간의 확산 촉진으로 123상이 단시간내에 생성되었고 입자성장도 촉진되었다. 발화합성법으로 제조한 시편은 기계적 혼합공정으로 제조한 시편에 비해 은 입자들은 미세하게 분산시킬 수 있어서 초전도체의 임계전류밀도가 향상되었다.

Abstract To obtain fine dispersion of Ag particles in $YBa_2Cu_3O_{7-y}$ (123) superconductors, 123 samples were made by pyrophoric synthetic method using malic acid and the subsequent solid-state reaction. As the pyrophoric synthetic powder was used as a precursor material, fine 123 powder of submicron size was produced in a short reaction time. The added Ag_2O was converted to metallic Ag during pyrophoric reaction and it accelerated both the formation of 123 phase and the grain growth via the enhanced mass transfer. The Ag particles of the sample sintered using the pyrophoric synthetic powder were more finely dispersed in the 123 matrix, compared to those of the sample sintered using the mechanically mixed powder, attributing to the improvement of the superconducting properties.

1. Introduction

The solid state reaction method, which involves a mechanical mixing of raw materials, calcination with an intermediate crushing, shape-forming and sintering, has been widely used for ceramic processing. This processing has been applied to the fabrication of the oxide superconducting materials. However, the critical current density (J_c) of $YBa_2Cu_3O_{7-y}$ (123) prepared by the conventional solid-state reaction method was very low.[1,2] One of the major causes for the low J_c is the weak-link property of the grain boundary that is an obstacle for the current travel.[3~5] Due to the high-energy state of the grain boundary, many inhomogeneities are, in general, concentrated at grain boundaries of a 123 phase. For example, barium carbonate ($BaCO_3$) and the liquid phase containing carbon are often present at the grain boundary, because of the slow decomposition of barium carbonate into BaO and CO_2.[6] In addition to the presence of the unreacted phases, improper mixing of raw materials can lead to the formation of the off-stoichiometric composition on 123 in the local parts of the powder, which forms the non-superconducting second phases during heat treatment.[7~11] If the local composition is barium-deficient, it induces a peritectic reaction and hence forms Y_2BaCuO_5 and a liquid phase,[9,11] lowering the melting point of the system.[9]

Compared to the mechanically mixed powder, chemically treated powder has a better chemical homogeniety. Many successful results have been achieved in the processes of coprecipitation,[12,13] spray pyrolysis,[14,15] citrate pyrophoric synthesis,[16~18] sol-gel,[19,20] aerosol flow reaction,[21] freeze drying method[22] and so on. Benefits of these processes are production of fine powder, good chemical homogeneity, short reaction time and low reaction temperature. Among the processes, the pyrophoric synthesis method is beneficial in mass production of powders and is a cost-effective method,[18] since the powder can be produced in a short time by explosive reaction as well as the oxides or carbonates that

were used as raw materials are cheap. Shieh et. al. reported that using of the citrate and nitrate precursor reduced the preparation time as well as lowered the formation temperature of a 123 phase.[18] The formation of single 123 phase was achieved below 690℃ in a helium atmosphere. Furthermore, this process allows forming the homogeneous aqueous solution of oxide materials with additives and dopants[17] and thus the intercalation of the dopants into the crystal lattice or the uniform dispersion of second phase particles in the superconducting matrix is easier.

Another effective way to improve the grain boundary property of the oxide superconductor is the addition of metallic element to the superconducting phase. Particularly, a metallic Ag phase is known to increase the J_c and the mechanical properties of the oxide superconductor via fine dispersion in the superconducting matrix.[23~28] Both Ag_2O and metallic Ag are used as an additive to a 123 phase without serious degradation of the superconducting properties, because the reaction between silver and 123 phase is not severe. The objective of this study is to achieve fine dispersion of mertallic silver in the 123 superconducting matrix using the pyrophoric synthetic powder as a precursor. Processing variables of the pyrophoric reaction and the superconducting properties of the prepared samples are reported.

2. Preparation of precursor powders

Precursor powders were made by pyrophoric synthetic method of Y_2O_3, $BaCO_3$ and CuO powder with and without 20 wt.% Ag_2O addition following the experimental procedure illustrated in Fig. 1. First, Y_2O_3, $BaCO_3$, CuO and 20 wt.% Ag_2O powders were weighed to a 123 composition and then the powder mixtures were dissolved in 1 N HNO_3 solution by using of a magnetic stirrer. The malic acid ($C_4H_6O_5$) was used for chelating with the ground powders. It has a structure containing COOH radicals that combine with metal ions (Ag^+, Ba^{+2}, Cu^{+2} and Y^{+3}) and then forms metal-organic complexes, $[Ag_2(C_4H_4O_5)]$, $[Ba(C_4H_4O_5)]$, $[Cu(C_4H_4O_5)]$ and $[Y_2(C_4H_4O_5)_3]$.

$$C_4H_6O_5+2Ag^+ \rightarrow [Ag_2(C_4H_4O_5)]+2H^+ \quad (1\text{-}1)$$

$$C_4H_6O_5+Ba^{+2} \rightarrow [Ba(C_4H_4O_5)]+2H^+ \quad (1\text{-}2)$$

$$C_4H_6O_5+Cu^{+2} \rightarrow [Cu(C_4H_4O_5)]+2H^+ \quad (1\text{-}3)$$

$$3C_4H_6O_5+2Y^{+3} \rightarrow [Y_2(C_4H_4O_5)_3]+6H^+ \quad (1\text{-}4)$$

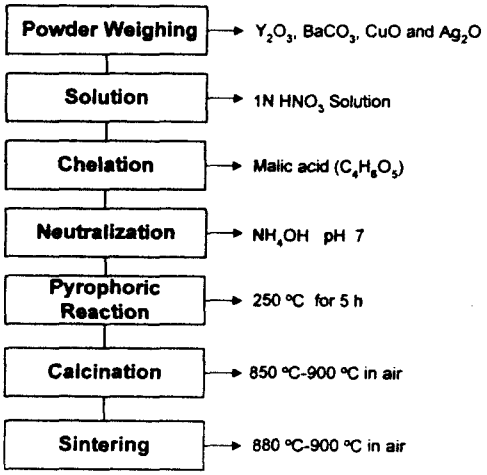

Fig. 1. Experimental procedure of pyrophoric synthetic method.

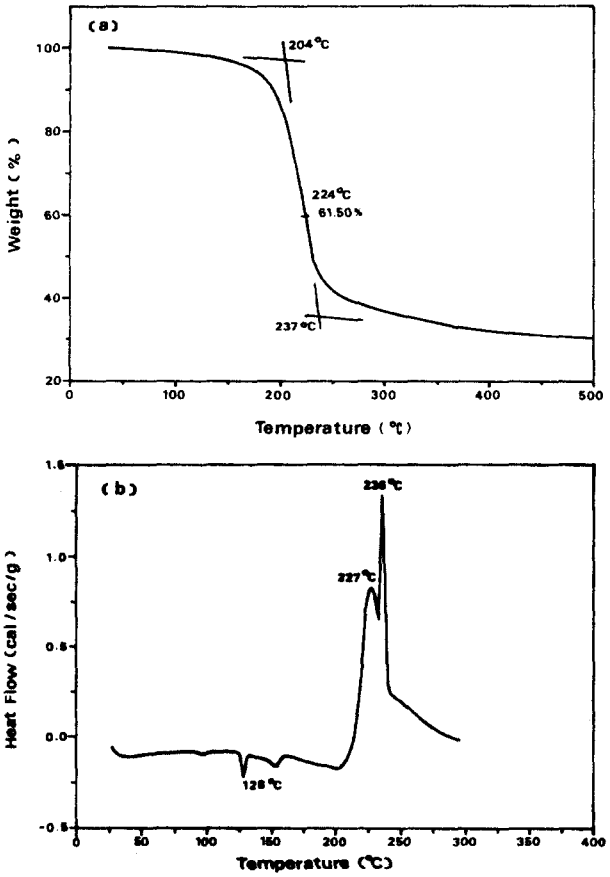

Fig. 2. TG (a) and DSC curve (b) of the powder neutralized and dried at 50℃.

After the complete dissolution of the powders, the associated amount of malic acid to the chelation ratios was added to the solution and then the solution was neutralized to PH=7 with ammonia water (NH_4OH).

In order to understand the heat events of the neutralized solution, thermogravimetric analysis (TGA) and differential scanning calorimeteric analysis (DSC) experimental were carried out for the powder neutralized and dried at 50℃, and the results were shown in Fig. 2.

As can be seen in the TG data (Fig. 2(a)), large mass change is observed near 225℃. It initiates near 200℃ and almost finishes near 240℃. In the DSC curve, there are two small exothermic peaks at 128℃ and 160℃, and the large double peaks at 227℃ and 236℃ (Fig. 2 (b)). The large mass change of the TG data and the large double DSC peaks implies that the violent exothermic reaction occurs around 230℃. This result is well consistent with the work by Bhattacharya et. al's[17] that reported the pyrophoric reaction at 225℃ in the precursor prepared using a citric acid ($C_6H_8O_7$). The bottle of the neutralized solution was, therefore, heated to 250℃ in an oven and then held at this temperature for 5 h. Holding at this temperature, the solution foamed and yielded fine powders of dark brown color. During heating, NH_4NO_3 in the neutralized solution decomposes into several gas phases following reaction and heat generates by the exothermic reaction.

$$2NH_4NO_3 \rightarrow 2NH_3 + H_2O + 2NO_2 + 1/2O_2 + Heat \quad (2)$$

Figure 3 is scanning electron micrograph (SEM) of the precursor powder without Ag_2O addition, prepared by pyrophoric synthetic method. The pyrophoric synthetic powder appears as a large agglomeration of the component powders and the size is a few tens of microns. Many pores are observed inside the powder, owing to the gas evolution during pyrophoric reaction. Not illustrated here, the morphology of the pyrophoric synthetic powder with Ag_2O addition was similar to that of Fig. 3.

Figure 4 shows powder X-ray diffraction patterns of the prepared precursor powders with (a) no addition and (b) 20 wt.% Ag_2O. In both patterns, all the peaks correspond to the patterns of the raw materials of Y_2O_3, $BaCO_3$ and CuO phase. Formation of a 123 phase during pyrophoric reaction was not observed. This means that during pyrophoric reaction, the metal-organic complexes were converted again into the metal oxides of Y_2O_3 and CuO and the carbonate of $BaCO_3$. It should be noticed that the peaks of metallic Ag are observed in the Ag_2O-doped powder precursor. It was reported that Ag_2O was converted into metallic Ag at 390℃ in air[27] and around 500℃ in O_2 atmosphere[28] in the presence of 123 phase. The observation of metallic Ag peaks of the XRD pattern of this study is due to the formation of the metallic Ag from the organic complexes of $[Ag_2(C_4H_4O_5)]$. However, it is not clear whether $[Ag_2(C_4H_4O_5)]$ is directly converted into metallic Ag phase during pyrophoric reaction or converted first into the intermediate

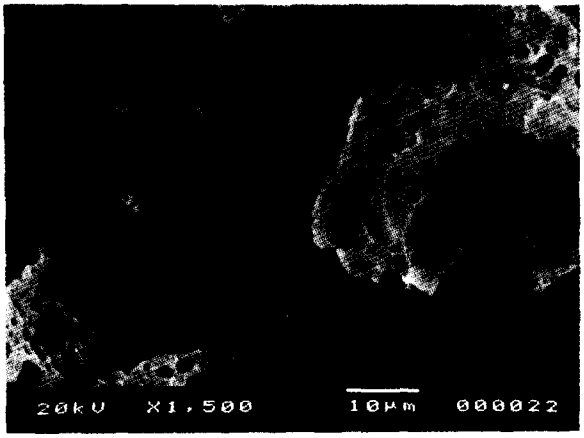

Fig. 3. SEM micrograph of the pyrophoric synthetic powder without Ag_2O addition.

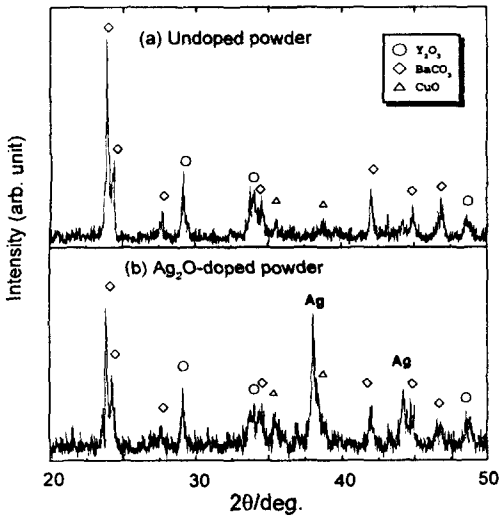

Fig. 4. Powder X-ray diffraction patterns of the pyrophoric synthetic powder with (a) no addition and (b) 20 wt.% Ag_2O.

phase of Ag_2O and finally metallic Ag. Even if Ag_2O forms during pyrophoric reaction, it will be tansformed to metallic Ag by the heat evolved during the exothermic reaction of eq. (2).

3. Formation of a 123 phase in the pyrophoric synthetic powder with and without Ag_2O addition

To know the formation of a 123 phase in the pyrophoric synthetic powders with no addition and 20 wt.% Ag_2O addition, 0.5 g of each powders were uniaxially pressed in a steel mold and made into 10 mm dia. compacts. The compacts were placed on alumina plates, heated to various temperatures of 850℃, 890℃ and 900℃ in air at a rate of 100℃/h, held for various time periods and then cooled to room temperature at a rate of 100℃/h.

Figure 5 shows powder XRD patterns of the samples

with (a) no addition and (b) 20 wt.% Ag_2O addition, heat-treated at 850℃ in air for 1 h. Although a large amount of the raw materials were converted to a 123 phase, peaks of the raw materials are still observed in both patterns. The peak intensity of $BaCO_3$, CuO and Y_2O_3 of sample (b) is relatively lower than that of sample (a).

Figure 6 shows powder XRD patterns of the sample with (a) no addition and (b) 20 wt.% Ag_2O addition, heat-treated at 900℃ in air for 1 h. At this temperature, the amounts of the formed 123 phase of both samples are larger than those formed at 850℃. Small $BaCO_3$ peak is still observed in the pattern of sample (a), while no impurity peaks in the pattern of sample (b). This indicates that the formation of the 123 phase in the sample with Ag_2O addition was faster than in the sample with no addition.

Figure 7 shows the variations of a volume fraction of a 123 phase as a function of a reaction temperature and time in an air atmosphere of the pyrophoric synthetic powders with (a) no addition and (b) 20 wt.% Ag_2O addition. It can be seen in both powders that the formation of the 123 phase is more sensitive to temperature than time. At 850℃, the formation reaction of a 123 phase was very slow, owing to the sluggish decomposition of $BaCO_3$.[6] The volume fraction of the 123 phase of sample (a), which were heat-treated at 850℃ for 0.5 h, 1 h, 5 h and 10 h, are 56 %, 65 %, 80 % and 90 %, respectively. As the reaction time increased to 880℃, the formed amount of the 123 phase increases to some extent but still slow. The volume fractions of the

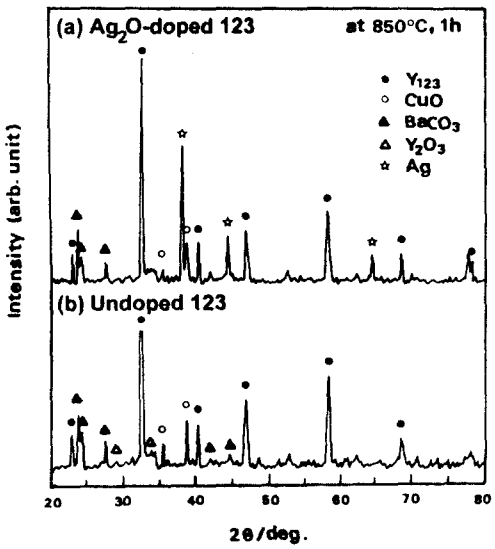

Fig. 5. Powder XRD patterns of the sample with (a) no addition and (b) 20 wt.% Ag_2O addition, heat-treated at 850℃ in air for 1 h.

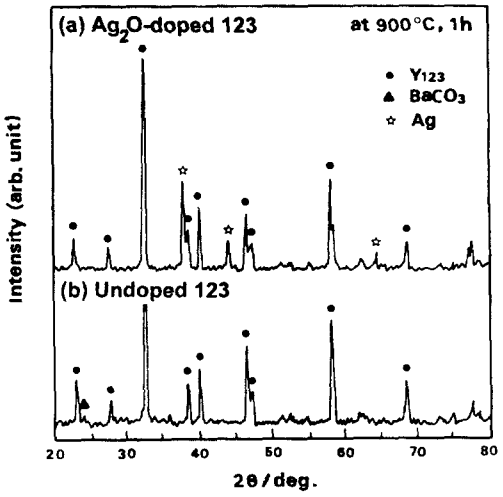

Fig. 6. Powder XRD patterns of the sample with (a) no addition and (b) 20 wt.% Ag_2O addition, heat-treated at 900℃ in air for 1 h.

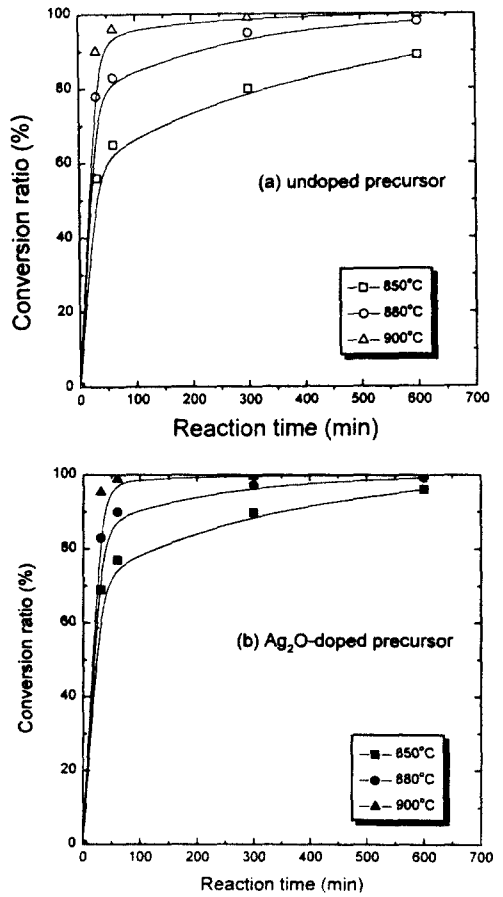

Fig. 7. Variation of a volume fraction of a 123 phase as a function of reaction temperature and time of the pyrophoric synthetic powder with (a) no addition and (b) 20 wt.% Ag_2O.

123 phase for 1 h and 10 h are 83 % 98.6 %, respectively. On the other hand, the formation of the 123 phase at 900℃ is very fast. The volume fraction of the 123 phase at 900℃ for 0.5 h, 1 h, 5 h and 10 h are 90 %, 97 %, 99.2 % and 99.9 %, respectively. This is

due to the fact that the eutectic liquid phase forms around 900℃[8,29] and then the liquid phase enhances the mass transfer for the formation of the 123 phase. However, the formation kinetics of the 123 phase of this study is much slower than that reported by Shieh et. al.[8] Referring to their result, the citrated precursor powder was completely converted to a 123 phase at the very low temperature of 690℃ within 1 h. Unlike to the air atmosphere of this study, their precursor powder was heat treated in a helium atmosphere. The enhanced 123 formation of their study may be mainly due to the fast oxygen diffusion in a helium atmosphere,[30] because the number of oxygen vacancy in the 123 phase in the inert atmosphere is larger than that in the air atmosphere.[31]

On the other hand, it can be seen in Fig. 7 (b) that the formation of a 123 phase in the precursor powder with Ag_2O addition was faster than that of the powder with no addition. At 850℃ for 10 h, the formed amount of a 123 phase is 96.2 % which is higher than 90% of the powder with no addition at the same reaction time. The volume fraction of the 123 phase at 880℃ for 0.5 h, 1 h, 5 h and 10 h are 83.2 %, 90.3 %, 97.4 % and 99.3 %, respectively. At 900℃, the formation of the 123 phase is very fast. 95 % of the precursor powder was converted into a 123 phase within 0.5 h. These results indicate that the formation of the 123 phase was accelerated by addition of Ag_2O to the precursor powder. The metallic Ag phase that was converted from Ag_2O during pyrophoric reaction seems to enhance the diffusion required for the formation of the 123 phase.

4. Particle size of a 123 phase and Ag distribution

Figure 8 shows SEM microstructure of the fractured surface of the samples prepared from the pyrophoric synthetic powder with no addition and 20 wt.% Ag_2O addition. Samples (a) and (b) were calcined at 880℃, and (c) and (d) at 900℃ for 5 h in an air atmosphere. The volume fractions of the 123 phase of both samples were larger than 95 %. The 123 particles of sample (a) are as fine as submicrons in size while those of sample (b) are as large as 23 microns and more anisotropic. At 900℃, significant grain growth of a 123 phase are observed. The particles of the sample with no addition are 2-3 microns in size but the particles of the sample with 20 wt.% Ag_2O addition are 3-5 microns (Figs. 8 (c) and (d)).

Figure 9 shows the particle size distribution of the sample calcined at 880℃ for 60 h with repeated grindings for every 20 h, using the pyrophoric synthetic powder with (a) no addition and (b) 20 wt.% Ag_2O addition. The mean diameters of samples (a) and (b)

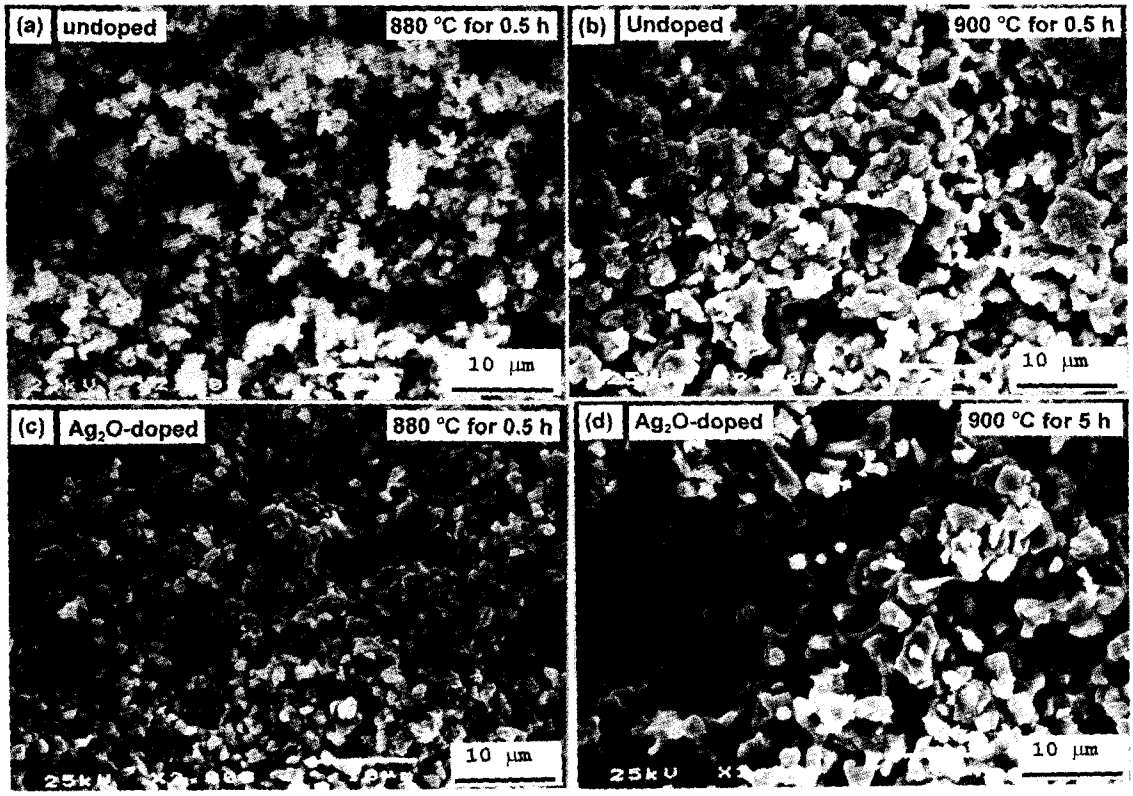

Fig. 8. SEM microstructures of the fractured surfaces of the samples with no addition and 20 wt.% Ag addition prepared from tl pyrophoric synthetic powders. Samples (a) and (b) were calcined at 880℃, and (c) and (d) at 900℃ for 5 h in an air atmosphere.

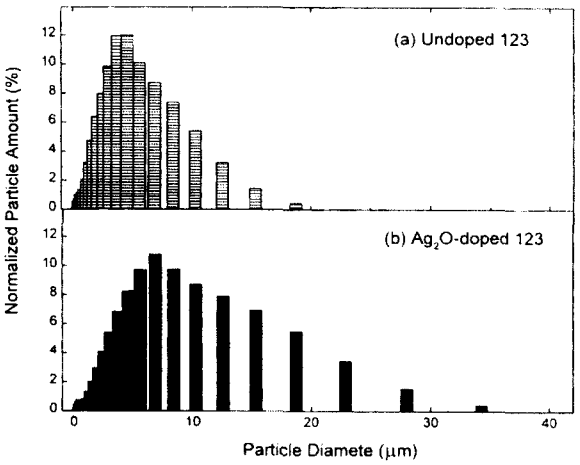

Fig. 9. Particle size distribution of the samples calcined at 880℃ for 60 h in air with repeated grindings for every 20 h, using the pyrophoric synthetic powder with (a) no addition and (b) 20 wt. % Ag_2O addition.

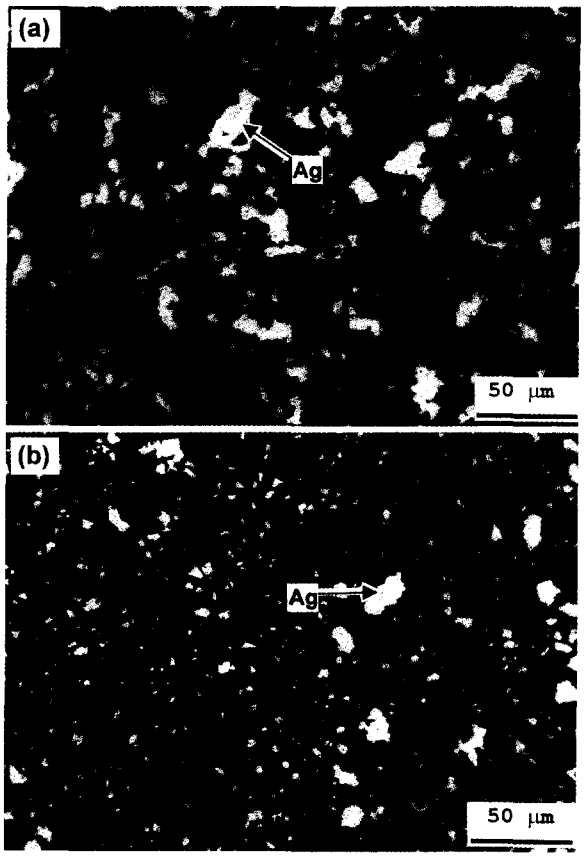

Fig. 10. Optical microstructure of the polished surfaces of the sample prepared from (a) mechanical mixed powder with Ag addition and (b) pyrophoric synthetic powder with Ag_2O addition. The bright and the dark phases are metallic Ag and pores, respectively.

are 3.6 microns and 4.6 microns, respectively. The large 123 particles in the sample with 20 wt.% Ag_2O addition is well consistent to other works that reported the enhancement of 123 grain growth in the 123-Ag_2O composite systems.[28, 32]

To understand the distribution of the metallic Ag phase in the sintered samples, the 123-Ag composite samples were made from two different precursor powders, the mechanically mixed powder with metallic Ag and the pyrophoric synthetic powder with Ag_2O addition. The mean diameter of the Ag particles used in the mechanically mixed powder was 5 microns. The Ag powder was mixed with Y_2O_3, $BaCO_3$ and CuO powders by ball milling in a zirconia jar and balls for 10 h using alcohol and then dried in air. Two precursor powders were calcined at 880℃ for 60 h, made into pellets, sintered at 900℃ for 10 h and then oxygenated at 500℃ for 40 h in flowing oxygen.

Figure 10 shows an optical microstructure of the polished surfaces of the sample prepared from (a) mechanical mixed powder with Ag addition and (b) pyrophoric synthetic powder with Ag_2O addition. It can be seen in both samples that the metallic Ag particles (the bright phases marked by arrows) are dispersed in the 123 matrix. Some of the pores are filled with metallic Ag phase. The size of the Ag particles of sample (a) is larger than its original size (5 microns), owing to the significant grain growth of metallic Ag phase during calcination and sintering. It should be noted that the size of the Ag particles of sample (b) is finer than that of sample (a) and the distribution is more uniform, although the large Ag particles are also observed. Furthermore, the amount of the porosity of sample (b) is relatively smaller than that of sample (a). This is due to the fact that the Ag_2O particles used in sample (b) were completely dissolved as an ionic form in a nitric acid solution and then they precipitated homogeneously in a fine particle form during heat treatment.

5. Superconducting properties

Figure 11 shows DC magnetization curves of the 123 samples with no addition and 20 wt. % Ag_2O addition prepared from the pyrophoric synthetic powders. The magnetization was measured for the powder samples by a commercial SQUID (superconducting quantum interference device) magnetometer (Quantum Design, MPMS). The samples were calcined at 880℃ for 60 h, sintered at 900℃ for 10 h in air and then oxygenated at 500℃ for 40 h in flowing oxygen. The onset temperatures of the superconducting transition of the samples with no addition and Ag_2O addition are 91.1 K and 91.2 K, respectively. The sample with no addition shows the second transition near 60 K, which may be caused by the insufficient oxygen diffusion in the sample. Com-

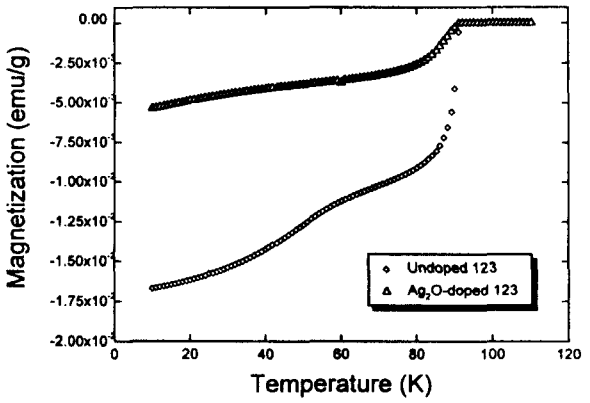

Fig. 11. DC magnetization curves of the 123 samples with no addition and 20 wt. % Ag_2O addition prepared pyrophoric synthetic powders. The samples were calcined at 880℃ for 60 h, sintered at 900℃ for 10 h in air and then oxygenated at 500 ℃ for 40 h in flowing oxygen.

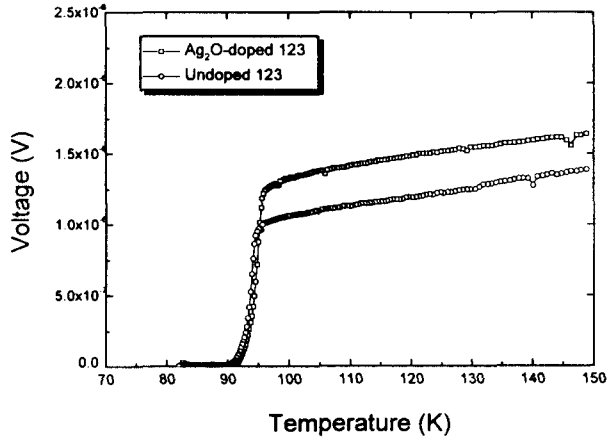

Fig. 12. Voltage-temperature curves of the 123 samples with no addition and 20 wt. % Ag_2O addition prepared pyrophoric synthetic powders.

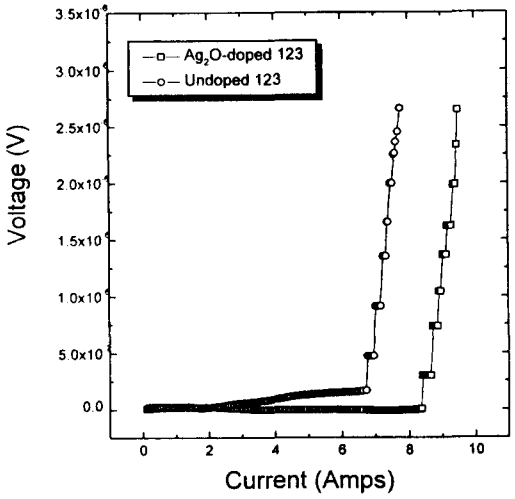

Fig. 13. Voltage-current curves at 77 K of the 123 samples with no addition and 20 wt. % Ag_2O addition prepared pyrophoric synthetic powders.

pared to that of the sample with no addition, the superconducting volume of the sample with Ag_2O addition is relatively low, which is due to the presence of non-superconducting Ag phase in the sample with Ag_2O addition.

Figure 12 shows voltage-temperature curves of the above samples estimated by the four probe methods using silver paste contacts. The zero-resistance temperatures of the 123 sample with no addition and with Ag_2O addition are 91 K and 90 K, respectively. The T_c values are well consistent with the magnetization data of Fig. 11.

Figure 13 shows the current-voltage curves at 77 K of the 123 samples with no addition and 20 wt. % Ag_2O addition prepared using the pyrophoric synthetic powders. Critical currents (I_c) of the samples with no addition and Ag_2O addition are 7.2 A and 8.9 A, respectively. The J_c values of the samples are 120 A/cm^2 and 150 A/cm^2, respectively. The small increase in J_c of this study seems to be attributed to the enhanced densification of 123 matrix and the fine dispersion of Ag particles.

6. Conclusions

In this study, fine $YBa_2Cu_3O_{7-y}$ (123) and $YBa_2Cu_3O_{7-y}$-Ag composite superconductors were fabricated by pyrophoric synthetic method using malic acid and the subsequent solid state reaction. The pyrophoric synthetic powder has several beneficial points in fabrication of the oxide superconductors. This process is cost-effective, since the types of the raw materials are oxides and carbonate forms of a cheap price. The use of the fine precursor powder allows the formation of a 123 phase in a shorter reaction time, compared to the use of a mechanically mixed powder using ball milling. The Ag_2O addition accelerated both the formation and the grain growth of the 123 phase via the enhanced mass transfer. In addition, the metallic Ag particles were more finely dispersed in the 123 matrix than those of the sample sintered using the mechanically mixed precursor. Superconducting transition temperature of the 123 and the 123-Ag composites were as high as 91 K. Critical current density of the 123 sample with 20 wt.% Ag_2O addition was higher than that of the 123 sample with no addition.

References

1. Y. Gao, Y. Li, K. L. Merkle, J. N. Mundy, C. Zhang, U. Balachadran and R. B. Poeppel, Mater. Lett., **9** 347 (1990)
2. Y. Masuda, R. Ogawa, Y. Kawate, K. Matsubara

and T. Tateishi, J. Mater. Res., **8** 693 (1993)
3. J. W. Ekin, Adv. Ceram. Mater., **2** 586 (1987)
4. J. A. Yarnoff, D. R. Clark, W. Drube, U. O. Karlson, A. Taleb-Ibrahimi and F. J. Himpsel, Phys. Rev., **B36** 3967 (1987)
5. S. Nakahara, G. J. Fisanick, M. F. Yan, R. B. van Dover, T. Boone and R. Moore, J. Cryst. Growth, **85** 639 (1987)
6. D. R. Clark, T. M. Shaw and D. Dimos, J. Amer. Ceram. Soc., **72** 1103 (1989)
7. J. E. Ullman, R. W. McCallum and J. D. Verhoeven, J. Mater. Res., **4** 753 (1989)
8. T. L. Aselage and Keefer, J. Mater. Res., **4** 1279 (1988)
9. T. L. Aselage, Physica C, 233 292 (1994)
10. C-J. Kim, K-B. Kim, I-H. Kuk and G-W. Hong, Mater. Sci. Eng., **B39** 25 (1996)
11. C-J. Kim, K-B. Kim, I-H. Kuk and G-W. Hong, Physica C, **255** 95 (1995)
12. D. H. Chen, T. W. Liu, J. Cc. Huang, C. H. Cheng, C. T. Chang, S. R. Sheen, T. C. Wang and M. K. Wu, Mater. Lett., **21** 15 (1994)
13. A. Bhargava, I. D. R. Mackinnon, Toru Yamashita and D. Page, Physica C, **53** (1995)
14. N. Tohge, M. Tatsumisago, T. Minami, K. Okuyama, M. Adachi and Y Kousaka, Jpn. J. Appl. Phys., **27** L1086 (1988)
15. C. H. Chao and P. D. Owinby, Mater. Sci., **30** 6236 (1995)
16. D. H. Blank, H. Kruidhof and J. Flokstra, J. Phys. D: Appl. Phys. **21** 226 (1988)
17. D. Bhattacharya, L. C. Pathak, S. K. Mishra, D. Sen and K. L. Chopra, J. Appl. Phys. Lett., **57** 2145 (1990)
18. S. H. Shieh and W. J. Thomson, Physica C, **204** 135 (1992)
19. N. E. Khokh, R. Papiernik, L. G. Hubert-Pfalzgraf, F. Chaput and J. P. Boilot, Mater. Sci. Lett., **8** 762 (1989)
20. Y. Masuda, R. Ogawa, Y. Kawate, K. Matsubaram, T. Tateishi and S. Sakka, J. Mater. Res., **7** 819 (1992)
21. T. T. Kodas, E. M. Engler, V. Y. Lee, R. Jacowitz, T. H. Baum, K. Roche, S. S. P. Parkin, W. S. Young, S. Highes, J. Kleder and W. Auser, Appl. Phys. Lett., **52** 1622 (1988)
22. Y. Kimura, T. Ito, H. Yoshikawa, T. Tachiwaki and A. Hiraki, Japan. J. Appl. Phys., **29** L1409 (1990)
23. L. S. Yeou and K. W. White, J. Mater. Res., **7** 1 (1992)
24. F. Yeh and K. W. White, J. Appl. Phys., **70** 4989 (1991)
25. J. Joo, J. P. Singh, R. B. Poeppel, K. Gangopadhyay and T. O. Mason, J. Appl. Phys., **71** 2351 (1992)
26. J. P. Shingh, H. L. Leu, R. B. Poeppel, E. V. Voorhees, G. T. Goudey, K. Winsley and D. Shi, J. Appl. Phys., **66** 3153 (1989)
27. A. Goyal, S. J. Burns and P. D. Funkenbusch, Physica **C168** 405 (1990)
28. T. H. Tiefel, S. Jin, R. C. Sherwood, M. E. Davis, G. W. Kammlott, P. K. Gallagher, D. W. Johnson Jr., R. A, Fastnacht and W. W. Rhodes, Mater. Lett., **7** 363 (1989)
29. W. Wong-Ng and L. P. Cook, J. Am. Ceram. Soc., **77** 1883 (1994)
30. J. J. Rha, K.Y. Yoon, S-J. L. Kang and D. N. Yoon, J. Am. Ceram. Soc., **71** 131 (1989)
31. P. K. Gallagher, Adv. Ceram. Mater., **2** 632 (1987)
32. J. J. Lin, T. M. Chen, Y. D. Yao, J. W. Chen and Y. S. Gou, Jpn. J. Appl. Phys., **29** 497 (1990)